

## Characterization by the Impedance Spectroscopy of $(\text{ZnO})_x(\text{CdO})_{(1-x)}$ Composite Thin Films

Halima BENATTOU, Nouredine BENRAMDANE,  
Kamel SAHRAOUI

Laboratoire d'Elaboration et Caractérisation des Matériaux,  
Djillali Liabes University, Sidi Bel-Abbes, Algeria  
Tel.: 00213792619048  
E-mail: h.benattou@gmail.com

Received: 31 December 2012 / Accepted: 10 August 2013 / Published: 26 May 2014

**Abstract:** The DC and AC electrical conduction of  $(\text{ZnO})_x(\text{CdO})_{(1-x)}$  thin films were investigated in this work. AC conductivity of  $(\text{ZnO})_x(\text{CdO})_{(1-x)}$  ( $X=0.2, 0.7$ ) thin films was reported in the frequency range 5 Hz to 13 MHz and at the temperature of 20 °C, 40 °C and 60 °C using impedance spectroscopy. The main results were presented by frequency dependence of complex impedance real and imaginary parts of the samples and by Nyquist diagrams at different temperatures. Thin films electrical properties were determined, proposing an equivalent circuits constituted by resistances and capacities. The relaxation times values of  $(\text{ZnO})_{(0.7)}(\text{CdO})_{(0.3)}$  films computed suggested two relaxation process. The AC conductivity dependence on frequency and temperature revealed that a correlated barrier hopping model of the AC conduction was the most probable process in  $(\text{ZnO})_{(0.7)}(\text{CdO})_{(0.3)}$  films. Furthermore the calculated dielectric constants depended on frequency and temperature. The interfacial and orientation polarization contributed to the enhancement of the dielectric response of the two composites. *Copyright © 2014 IFSA Publishing, S. L.*

**Keywords:** Complex impedance spectroscopy, Thin films, ZnO, CdO, AC conductivity.

### 1. Introduction

The composite materials investigation started more than one century ago. The efforts to design a new product did not stop because of the particular interest related to these materials. The major interest was the possibility to obtain a diverse properties according to the constitute phases characteristics. The applications of these materials were especially in the electronic engineering fields such as transparent conducting materials as oxides in thin films. They had an electrical conductivity and an optical transparency satisfactory for the modern technological applications (like transparent electrodes in solar cells, screens with liquid crystals). It results a strong demand for dielectric materials with well

defined properties and materials transparent to the electromagnetic waves in defined wavelengths ranges. However the natural materials properties generally do not satisfy the modern requirements of industry. Artificial materials having at the same time a larger gap, high transparency, high permittivity and high conductivity were then used in the objective to meet these needs. The cadmium oxide and the Zinc oxide are two materials which belong to transparent conducting oxides (TCO), of group II-VI of the semiconductors. Both are n-type semiconductor components [1, 2]. The band gap energy of the ZnO is 3.3eV [3, 4]. Its resistivity is in the order of  $10^3 \Omega \cdot \text{cm}$  [5]. The zinc oxide in thin films is used in variety of applications such as: Electronic systems like varistors employed at the time of large cuts of

voltage [6]; Fields of optoelectronics and electroluminescence [7]; Sensor of chemicals in thin films. CdO thin films have band gap energy about 2.3 eV [8-10]. Its resistivity is in the order of  $10^{-2} \Omega \cdot \text{cm}$  [11] at ambient temperature. CdO thin films are used in the photodiodes, Phototransistors, Photovoltaic cells, transparent electrodes, the detectors IR.

For the ZnO and CdO applications mentioned above, we were interested in this work in the electrical and dielectrical properties study of the two materials ZnO and CdO composition. We used the impedance spectroscopy technique for the investigating of their properties in AC current. This experimental technique is based on the electrical response analysis of the system to a perturbing electrical action with an alternating frequency [12, 13].

## 2. Experimental Details

The films were deposited by chemical Spray Pyrolysis technique, their thickness were in the order of  $0.5 \mu\text{m}$  after the deposition. While, the DC resistivity measurements were carried out using two points method in the ambient temperature. The dielectric characterization in AC current were done using an experimental banc of measure consisting of an impedance meter of the type HP4192 operating in the frequency range 5 Hz-13 MHz connected to the silver lacquer electrodes with a coplanar configurations. The AC analyzer was driven by a computer using a LABVIEW program to sweep the frequency of excitation from 5 Hz to 13 MHz at the temperature of  $20^\circ\text{C}$ ,  $40^\circ\text{C}$  and  $60^\circ\text{C}$ .

Measurements of the complex impedance in absolute value  $|z|$  and the phase angle  $\theta$  directly, were taken from the impedance meter. The electric impedance  $\tilde{z}(\omega)$ , in complex form, is expressed by

$$\tilde{z}(\omega) = z'(\omega) - i * z''(\omega), \quad (1)$$

$\tilde{z}(\omega)$  can be represented by:

1) The imaginary part versus real part ( $z''$  vs.  $z'$ ), i.e. Nyquist diagram.

2) Real and imaginary part versus the frequency:  $z'$  vs.  $\omega$ ,  $z''$  vs.  $\omega$ .

Comparing these curves to those of equivalent electrical circuit using the basic electrical circuits models in literature [14], [15]. The values of the constitute elements of the electrical circuits (resistance and capacity) can be determined by the fitting of the curves.

## 3. Results and Discussion

### 3.1. DC Electrical Conduction

To determine the resistivity of the sample, the two point method was used. Measurement of the resistivity was done using the Ohm's law. The

current value was taken crossing the film and the potential difference between two points in the film. The resistivity of the samples is given by the formula:

$$R = \frac{\rho * L}{S} = \frac{\rho * L}{W * d} = \left(\frac{1}{\sigma}\right) * \left(\frac{L}{W * d}\right), \quad (2)$$

Conductivity is given by the following expression:

$$\sigma = \left(\frac{L}{W * d}\right) * \left(\frac{1}{R}\right), \quad (3)$$

where  $\sigma$  is the conductivity of film; R is the resistance; W is the length of the electrode ( $0.5 \text{ cm}$ ); d is the thickness of the sample to be characterized ( $0.5 \mu\text{m}$ ); L is the distance between the two electrodes ( $1 \text{ cm}$ ); S is the electrode area ( $S = W * d$ ).

According to Table 1 we notice the following inequalities for resistances of the films at the ambient temperature:

$$R(x=0.7) > R(x=0.5) > R(x=0.3) > R(x=0.2) > R(x=0.1).$$

The films rich in Zinc oxide are more resistive, this resistivity starts to decrease when the cadmium oxide concentrations increases in the solution and of this fact conductivity increases too.

**Table 1.** Electrical parameters in D.C. current of  $(\text{ZnO})_x(\text{CdO})_{(1-x)}$  ( $X = 0.1, 0.2, 0.3, 0.5, 0.7$ ) thin films.

Sample	R [ $\Omega$ ]	$\rho$ [ $\Omega \cdot \text{cm}$ ]	$\sigma$ [ $\Omega^{-1} \cdot \text{cm}^{-1}$ ]
$(\text{ZnO})_{(0.1)}(\text{CdO})_{(0.9)}$	333.33	0.01667	60
$(\text{ZnO})_{(0.2)}(\text{CdO})_{(0.8)}$	1103.14	0.05516	18.13
$(\text{ZnO})_{(0.3)}(\text{CdO})_{(0.7)}$	$1.14 \times 10^6$	57.33945	0.017
$(\text{ZnO})_{(0.5)}(\text{CdO})_{(0.5)}$	$2.73 \times 10^6$	136.9863	0.0073
$(\text{ZnO})_{(0.7)}(\text{CdO})_{(0.3)}$	$4.95 \times 10^6$	247.52475	0.00404

The curve of the Fig. 1 shows a hop of resistivity for a composition higher than 20 %.

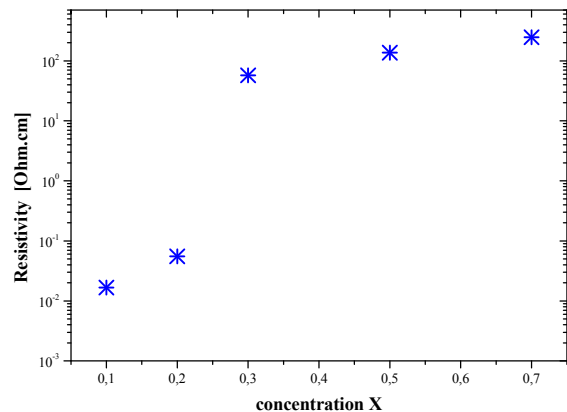


**Fig. 1.** Electrical resistivity plots versus the concentration X' in  $(\text{ZnO})_x(\text{CdO})_{(1-x)}$  ( $X = 0.1, 0.2, 0.3, 0.5, 0.7$ ).

Indeed, we note a change of conductivity for a volume of 20 % of zinc oxide. From a volume of 20 % of the CdO; the conductivity of the films is completely modified. Transport is not done more by CdO, because crystallites of this compound start to be separated by those of ZnO. We are in the case of heterogeneous material in which conducting crystallites separated by those insulating of ZnO. The theory predicts a volume of 20 % of conducting material in insulator to produce a percolation, i.e. a particular path for the electrical transport, which is not controlled any more by insulating crystallites [16].

### 3.2. AC Electrical Conduction

#### 3.2.1. The Response of the $(\text{ZnO})_{(0.2)}(\text{CdO})_{(0.8)}$ Sample

The curves of the Fig. 2 (b) represent The Nycquist diagram of the complex impedance of  $(\text{ZnO})_{(0.2)}(\text{CdO})_{(0.8)}$  composite, these curves are vertical lines at each temperature. They can be modeled as an equivalent electrical circuit constituted by a resistance in series with a capacity (Fig. 2a).

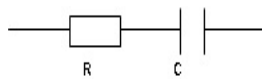


Fig. 2 (a). Equivalent electrical circuit of the  $(\text{ZnO})_{(0.2)}(\text{CdO})_{(0.8)}$  sample.

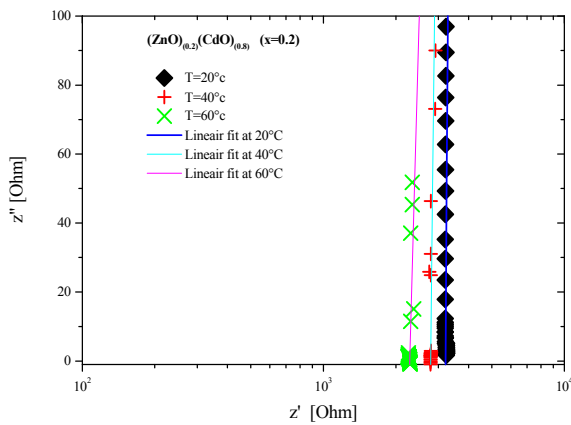


Fig. 2 (b). Nycquist diagram of the complex impedance of the  $(\text{ZnO})_{(0.2)}(\text{CdO})_{(0.8)}$  sample.

In the Fig. 3, the real part of the complex impedance of the  $(\text{ZnO})_{(0.2)}(\text{CdO})_{(0.8)}$  sample which represents resistance (R), is independent of the frequency. The resistance decreases with the increase in the temperature. The imaginary part of the complex impedance represents the capacity (C), it decreases with the increase of the frequency (Fig. 4). It is clear that the capacity varies according to the theory [14, 15], which confirms the coherent electric model to represent the film in this composition. The

fitting of the curves of  $z''$  and  $z'$  versus the frequency, gives us the resistance and the capacity values in Table 3.

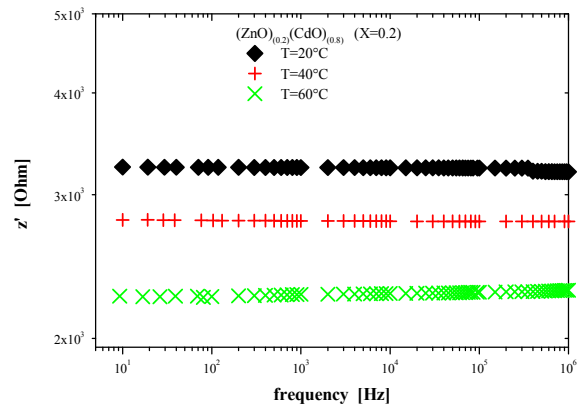


Fig. 3. Variation of the real part of the complex impedance versus the frequency of the  $(\text{ZnO})_{(0.2)}(\text{CdO})_{(0.8)}$  sample.

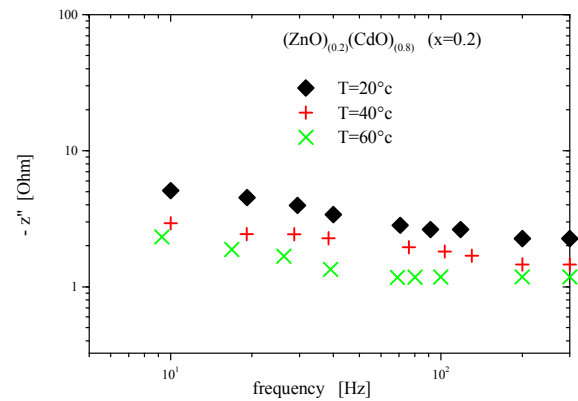


Fig. 4. Variation of the imaginary part of the complex impedance versus the frequency of  $(\text{ZnO})_{(0.2)}(\text{CdO})_{(0.8)}$  sample.

#### 3.2.2. The Response of the $(\text{ZnO})_{(0.7)}(\text{CdO})_{(0.3)}$ Sample

The Nycquist diagram of the complex impedance (Fig. 5b) is characterized by the presence of two semicircles at all temperatures; the first in the low frequencies and the second in the high frequencies. Each semicircle indicates the presence of a relaxation process. The diameters of the two semicircles are larger at the ambient temperature, it decreased when the temperature increased. This can suggests a thermally activated process. The two semicircles are modeled by an equivalent circuit consisting of two parallel circuits:  $(R_1C_1)$  and  $(R_2C_2)$  connected in series as shown in Fig. 5a. This model includes two relaxation times:

$$\tau_1 = R_1 * C_1, \tag{4}$$

$$\tau_2 = R_2 * C_2, \quad (5)$$

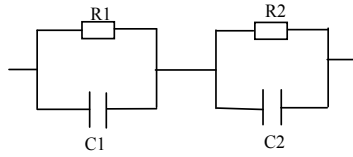


Fig. 5 (a). Equivalent electrical circuit of the (ZnO)<sub>0.7</sub>(CdO)<sub>0.3</sub> thin films into alternate current.

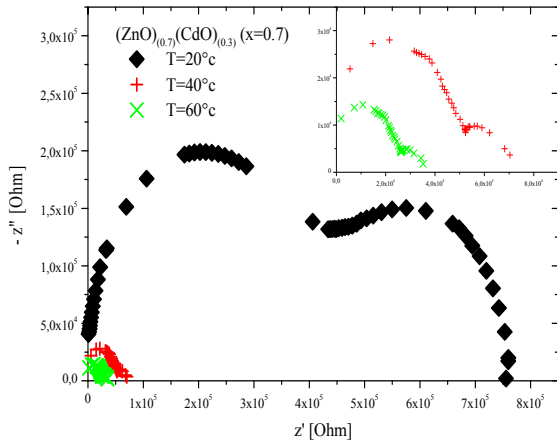


Fig. 5b. Nycquist diagram of the complex impedance of the (ZnO)<sub>0.7</sub>(CdO)<sub>0.3</sub> sample.

To confirm the obtained results, the variations of the imaginary and real parts versus the frequency are represented in Fig. 6 and Fig. 7 respectively.

The curves of impedance imaginary part spectrum in Fig. 6 reveal two different peaks at each temperature, this indicate the presence of two processes of relaxation each one is characterized by a relaxation frequency

$$f_1 = \frac{1}{2 * \pi * R_1 * C_1}, \quad (6)$$

$$f_2 = \frac{1}{2 * \pi * R_2 * C_2}, \quad (7)$$

which corresponds to the frequencies of the peaks in impedance imaginary part spectrum plot. The peaks satisfy the condition

$$\omega_1 * \tau_1 = 1, \quad (8)$$

$$\omega_2 * \tau_2 = 1, \quad (9)$$

then

$$\tau_1 = \frac{1}{2 * \pi * f_1}, \quad (10)$$

$$\tau_2 = \frac{1}{2 * \pi * f_2}, \quad (11)$$

where  $\omega_1$ ,  $\omega_2$  are the angular frequencies and  $\tau_1$ ,  $\tau_2$  are the relaxation times, one can evaluate the values of these parameters directly from impedance imaginary part spectrum plot (Fig. 6).

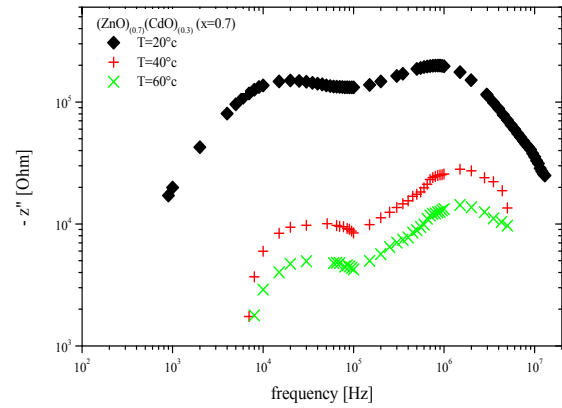


Fig. 6. Variation of the complex impedance imaginary part versus the frequency of the (ZnO)<sub>0.7</sub>(CdO)<sub>0.3</sub> sample.

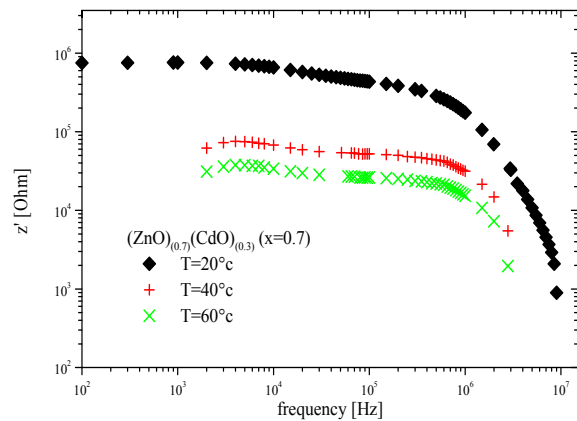


Fig. 7. Variation of the complex impedance real part versus the frequency of the (ZnO)<sub>0.7</sub>(CdO)<sub>0.3</sub> sample.

The values of parameters are shown in Table 2. In general way, we note a reduction in the relaxation time when the temperature increases. These relaxation times are attributed in the typical mechanisms of polarization: of orientation, interfacial or atomic. In the representation of The Nycquist diagram of the complex impedance (Fig. 5b), the response of the sample in high frequency (the first arc of semicircle) characterized by R<sub>1</sub> and C<sub>1</sub> where R<sub>1</sub> and C<sub>1</sub> are the contribution of resistance R<sub>g</sub> and the capacity C<sub>g</sub> of the grains respectively. The response in low frequency (the second arc of semicircle) characterized by R<sub>2</sub> and C<sub>2</sub> where R<sub>2</sub> and C<sub>2</sub> represent the contribution of resistance R<sub>gb</sub> and the capacity C<sub>gb</sub> of the grain boundaries respectively [17, 18]. The values of R<sub>g</sub>, C<sub>g</sub>, R<sub>gb</sub> and C<sub>gb</sub> are estimated by the

fitting which gave the following results in Table 3. At all temperatures (20 °C, 40 °C and 60 °C) the resistance of the grains is lower than that of the grain boundaries. These Results revealed that (ZnO)<sub>(0.7)</sub>(CdO)<sub>(0.3)</sub> composite is polycrystalline films.

**Table 2.** Relaxation times of the (ZnO)<sub>(0.7)</sub>(CdO)<sub>(0.3)</sub> sample.

T=20 °C		T=40 °C		T=60 °C	
$\tau_1$ [Sec] $\times 10^{-5}$	$\tau_2$ [Sec] $\times 10^{-5}$	$\tau_1$ [Sec] $\times 10^{-5}$	$\tau_2$ [Sec] $\times 10^{-5}$	$\tau_1$ [Sec] $\times 10^{-5}$	$\tau_2$ [Sec] $\times 10^{-5}$
0.81	0.02	0.52	0.0106	0.46	0.0078

**Table 3.** Estimated values of resistances and capacities: R<sub>g</sub>, C<sub>g</sub>, R<sub>gb</sub> and C<sub>gb</sub> of the (ZnO)<sub>(0.7)</sub>(CdO)<sub>(0.3)</sub> sample.

T °C	R <sub>g</sub> [Ω]	C <sub>g</sub> [Farad] $\times (10^{-12})$	R <sub>gb</sub> [Ω]	C <sub>g</sub> [Farad] $\times (10^{-12})$
20 °C	330865	0.2353	394328.5	48.46
40 °C	15205.83	0.021225	55609.07	1.8976
60 °C	7619.368	0.0407	29004.15	3.3879

The temperature has an effect on the relaxation frequency. The in-homogeneous of materials can be at the origin of this type of behavior. For impedance imaginary part spectrum plot (Fig. 6), one notices a displacement of the peak of relaxation towards the low frequencies with variation of the temperature.

### 3.3. Conductivity Study of the Composite Films

Conductivity in AC current ( $\sigma_{AC}$ ) calculated from the complex impedance using relation (12):

$$\tilde{\sigma} = \frac{1}{\tilde{\rho}} = \frac{1}{\tilde{z}} * \frac{L}{W * d}, \quad (12)$$

where  $\tilde{z}$  is the complex impedance; W is the length of the electrode; d is the thickness of the sample to be characterized, and L is the distance between the two electrodes.

In the general case, investigation of materials having various natures showed a universal behavior of conductivity:

1. A value of conductivity independent of the frequency until a breaking value.

2. A region in high frequency where conductivity has a monotonous increase.

For the (ZnO)<sub>(0.2)</sub>(CdO)<sub>(0.8)</sub> composite, there is a conducting behavior or composite semiconductor of thin films. Indeed, AC conductivity versus the frequency plots is independent of the frequency (Fig. 8). In this case, there is no critical frequency of the change of mechanism of conductivity where conductivity is independent of the frequency for:

$$\omega < \omega_c : \sigma(\omega < \omega_c) = \sigma_{AC}. \quad (13)$$

Different theoretical models have been developed to explain the frequency and temperature dependence of AC conduction in materials [19, 20]. In consequence of the excitation, the charge carrier transport between located states, due to the effects of the disorder in the films [21].

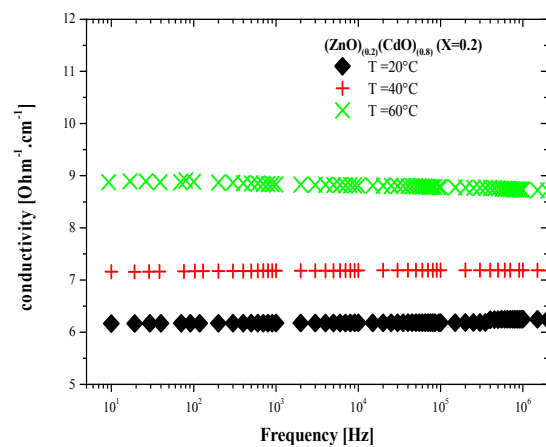


**Fig. 8.** Real part of conductivity versus the frequency and temperature of (ZnO)<sub>(0.2)</sub>(CdO)<sub>(0.8)</sub> thin films.

For the film with strong concentration of ZnO (i.e. (ZnO)<sub>(0.7)</sub>(CdO)<sub>(0.3)</sub>), in the high frequencies range ( $\omega > \omega_c$ ), one notes a typical variation of disordered materials. It is the case of a disordered materials behavior where transport of charge carriers takes place by hop between the even random distributed sites [22]. According to the universal power law of Jonscher expressed by formula (14):

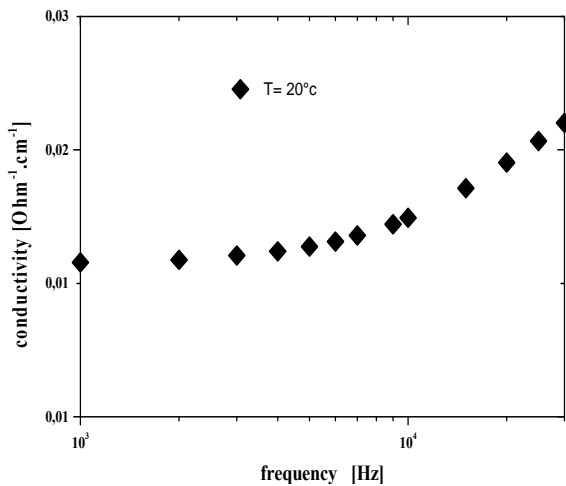
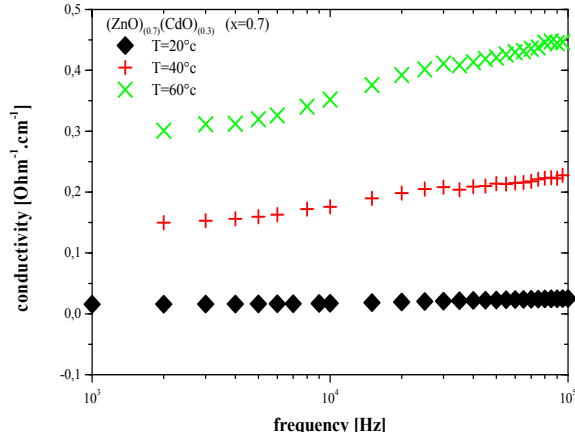
$$\sigma_{AC}(\omega) = A * \omega^S, \quad (14)$$

The exponent S is the temperature dependent ( $0 < S < 1$ ), A is the constant, and  $\omega$  is the angular frequency. The dependence of S on temperature is a function of the conduction mechanism [22]. On Table 4 we estimated the value of S from Fig. 9 using the logarithm of the equation (14) [23-25].

$$S = \frac{d \log(\sigma_{AC})}{d \log(f)} \quad (15)$$

**Table 4.** The values of S calculates at the temperatures of T=20 °C, 40°C and 60 °C.

	Exponent S		
	T=20 °C	T=40 °C	T=60 °C
(ZnO) <sub>(0.7)</sub> (CdO) <sub>(0.3)</sub>	0.165	0.157	0.122

**Fig. 9.** Real part of conductivity versus the frequency and temperature of (ZnO)<sub>(0.7)</sub>(CdO)<sub>(0.3)</sub> thin films.

The parameter S is the slope of the linear part of the curves of Fig. 9 with log representation in high frequencies range. The exponent S depends on the temperature. It decreases as the temperature increases from 0.165 at 20 °C to 0.122 at 60 °C. This decrease is in accordance with the assumption of thermally activated hop.

The exponent S decreases as the temperature increases as suggests that model *CBH* (Correlated Barrier Hopping) is the probable mechanism of electrical conduction in AC current. This model is one of the models used to describe the behavior of conductivity in alternating current through the parameter S. The model *CBH* describes a simultaneous hop of two electrons over the potential barrier separating from the R distant location [26]. In this model, S decreases with the temperature. Thus the variation of S with the temperature helps us to

identify the conduction mechanism. The characteristic of the model *CBH* is that the magnitude of S at a temperature was determined by the energy  $W_M$  of the charge carriers in their sites of localization.

According to the *CBH* model exponent S must obeys the formula:

$$S = 1 - \frac{6 * k_B * T}{W_M - k_B * T * \ln(1/\omega * \tau_0)}, \quad (16)$$

$$S = 1 - \frac{6 * k_B * T}{E_g}, \quad (17)$$

The expression  $W_M - k_B * T * \ln(1/\omega * \tau_0)$  represents energy ( $E_g$ ) necessary to cross the barrier.  $W_M$  is energy necessary to bring two electrons of fundamental state localized in potential wells to the free state in the conduction band [27, 28].  $\tau_0$  is the relaxation time which is in order of the vibrational period of the atoms ( $\tau_0 \approx 10^{-13}$  sec)  $k_B$  is the Boltzmann constant ( $k_B = 1.38 \cdot 10^{-23}$  J.K<sup>-1</sup>) and T is the temperature in Kelvin. For the large values of ( $W_M/k_B * T$ ), S is close to unity.

### 3.4. Complex Permittivity Study

The complex permittivity of two composite materials is studied versus the frequency in range 5 Hz - 13 MHz and at temperature of 20 °C, 40 °C and 60 °C. One computes the complex permittivity from the complex impedance using the following formulas:

$$\tilde{\epsilon} = \frac{\tilde{\sigma}}{i * \omega * \epsilon_0}, \quad (18)$$

where  $\tilde{\sigma}$  is the conductivity in AC current given by equation (12).  $\epsilon_0$  is the absolute permittivity of free space ( $\epsilon_0 = 8.85 \times 10^{-12}$  Farad/m).

Fig. 10 shows the real part of the complex permittivity plot versus the frequency at different temperatures. The large values of the real part of the complex permittivity towards the low- frequencies range are attributed to the interfacial polarization and, relaxation polarization due to the hopping of charge carriers which is very high in nanostructured materials. The loads accumulate at the two mediums interface (CdO and ZnO) when migrated under the influence of an electric field which results in the interfacial polarization [29-31].

These values decreases, it corresponds to the reduction in the material capacity to polarize (to stock electrical energy).

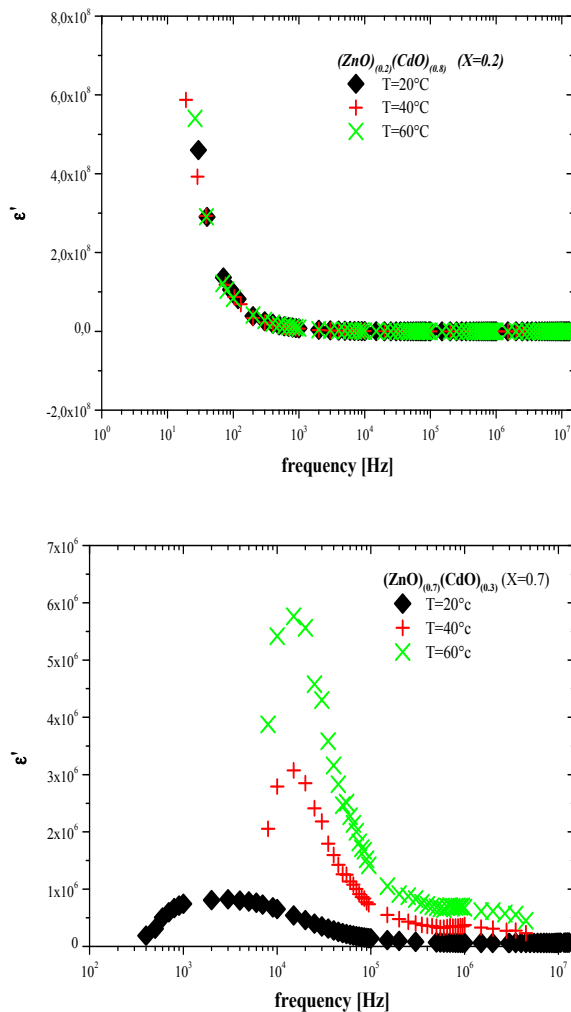


**Fig. 10.** The real part of the complex permittivity versus the frequency at different temperatures.

The real part of the permittivity increases with increasing temperature. In consequence the relaxation frequency of dispersion increases with increasing temperature.

The polarization is related to the electrons thermal motion when the temperature increases. It facilitates the orientation of the electrons [32].

## 6. Conclusions

The DC, AC electrical conductivity and complex permittivity of  $(\text{ZnO})_X(\text{CdO})_{(1-X)}$  ( $X=0.2, 0.7$ ) composite thin films have been investigated. The measured resistivity in DC conduction showed that the zinc oxide sample was very resistive than cadmium one's. It decreases with the increase of the cadmium oxide in material. In AC conduction the impedance spectroscopy analysis suggests that  $(\text{ZnO})_{0.2}(\text{CdO})_{0.8}$  film has a semiconductor behavior in which the electrical conduction of the charges is carried out between located states, due to the disorder effects in the films. The  $(\text{ZnO})_{0.7}(\text{CdO})_{0.3}$  composite was a polycrystalline

films consisting of the grains and the grain boundaries.

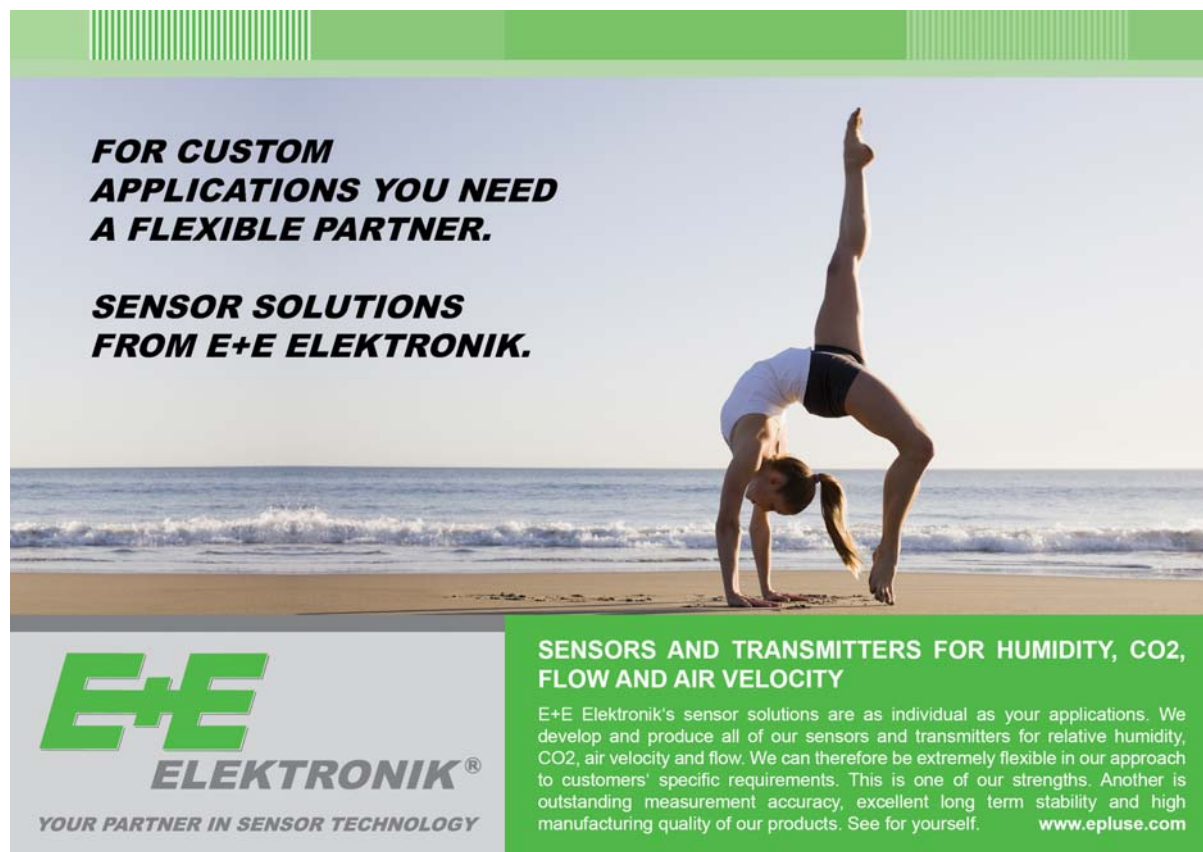
The AC conductivity of  $(\text{ZnO})_{0.7}(\text{CdO})_{0.3}$  thin films was found to be obey to the universal power law  $S$ . The decrease of the exponent  $S$  with temperature from 0.165 to 0.122 suggested that the correlated barrier hopping (CBH) model is the probable conduction mechanism to explain the electrical transport phenomenon. The dielectric measurements revealed that both interfacial and orientation polarizations were responsible for the enhancement of the dielectric properties of the  $(\text{ZnO})_X(\text{CdO})_{(1-X)}$  ( $X=0.2, 0.7$ ) composite thin films.

## References

- [1]. R. Ferro, J. A. Rodriguez, O. Vigil, Chemical composition and electrical conduction mechanism for CdO:F thin films deposited by spray pyrolysis, *Materials Science and Engineering: B*, Vol. 87, 2001, pp. 83-86.
- [2]. R. E. Hummel, Electronic properties of materials, Third Edition, *Springer*, 2000, pp. 178.
- [3]. S. Tewari, A. Bhattacharjee, P. P. Sahay, Studies on AC conductivity of spray deposited ZnO thin films, *Physical Sciences and Technology*, Vol. 5, No. II, 2010, pp. 216-219.
- [4]. B. Ergin, E. Ketenci, F. Atay, Characterization of ZnO films obtained by ultrasonic spray pyrolysis technique, *International Journal of Hydrogen Energy*, Vol. 34, 2009, pp. 5249–5254.
- [5]. Ü. Özgür, Ya. I. Alivov, C. Liu, A. Teke, M. A. Reshchikov, S. Doğan, V. Avrutin, S. J. Cho and H. Morkoç, A comprehensive review of ZnO materials devices, *Journal of Applied Physics*, Vol. 98, 2005, pp. 041301.
- [6]. R. N. Viswanath, S. Ramasams, R. Ramanoorthy, P. Jayavel, T. Nagarajan, Preparation and characterization nanocrystalline ZnO based materials for varistor applications, *Nanostructured Materials*, Vol. 6, 1995, pp. 993-996.
- [7]. T. Pauporté, D. Lincot, Electrodeposition of semiconductors for optoelectronic devices: results on zinc oxide, *Electrochimica Acta*, Vol. 45, 2000, pp. 3345 - 3353.
- [8]. B. J. Lokhande, P. S. Patil, M. D. Uplane, Studies on cadmium oxide sprayed thin films deposited through non aqueous medium, *Materials Chemistry and Physics*, Vol. 84, 2004, pp. 238-242.
- [9]. M. D. Uplane, P. N. Kshirsagar, B. J. Lokhande, C. H. Bhosale, Characteristic analysis of spray cadmium oxide thin films, *Materials Chemistry and Physics*, Vol. 64, 2000, pp. 75-78.
- [10]. K. Ouari, N. Benramdane, Z. Kebbab, A. Nakrela, R. Desfeux, Theoretical and experimental study of CdO, *Journal of Active and Passive Electronic Devices*, Vol. 7, 2012, pp. 29-37.
- [11]. K. Gurumurgan, D. Mangalaraj, Sa. K. Narayandass, Characterization of cadmium oxide thin films deposited by spray pyrolysis, *Journal of Crystal Growth*, Vol. 147, 1995, pp. 355-360.
- [12]. V. V. Tomaev, V. P. Miroshkin, V. P. Miroshkin, L. N. Gar'kin, A. Yu. Zhivago, Impedance Spectroscopy of Metal-Oxide Nanocomposites, *Glass Phys. Chem*, Vol. 30, Issue 5, 2004, pp. 624–637.

- [13]. V. V. Tomaev, V. P. Miroshkin, L. N. Gar'kin, P. A. Tikhonov, Dielectric Properties and Phase Transition the PbSe + PbSeO<sub>3</sub> Composite Material, *Fiz. Khim. Stekla*, Vol. 31, Issue 6, 2005, pp. 1117–1127.
- [14]. E. Barsoukov, J. Ross Macdonald, Fundamentals of impedance spectroscopy, in Impedance Spectroscopy: Theory, Experiment, and Applications 2<sup>nd</sup> Edition, *John Wiley & Sons*, 2005.
- [15]. P. Dzwonkowski, Micro-générateur électrochimique Li/B<sub>2</sub>O<sub>3</sub> + X-LiO<sub>2</sub>/InSe, thèse de doctorat, *Université Pierre et Marie Curie*, 1990.
- [16]. S. R. Broadbent, J. M. Hammersley, Percolation processes I. Crystals and mazes, *Proc. Cambridge Phil. Soc.*, Vol. 53, 1957, pp. 629–641.
- [17]. A. Broniatowsky, Cr Colloque de joints de grains dans les matériaux, *Carry-Le-Rouet*, France, 1984.
- [18]. K. Prabakar, Sa. K. Narayandass, D. Mangalaraj, Dielectric studies on Cd<sub>0.4</sub>Zn<sub>0.6</sub>Te thin films, *Materials Chemistry and Physics*, Vol. 78, 2003, pp. 809-815.
- [19]. D. K. Ambroise, Contribution à l'étude des propriétés électroniques de quelques brais de houille, Thèse de doctorat, *Université des Sciences et Techniques du Languedoc*, 1989.
- [20]. M. Pollak, G. E. Pike, AC conductivity of glasses, *Phys. Rev. Lett.*, Vol. 28, 1972, pp. 1449-1451.
- [21]. P. W. Anderson, Absence of diffusion in certain random lattices, *Phys. Rev.*, 1958.
- [22]. A. Madan, M. P. Shaw, The Physics and applications of amorphous semiconductors, *Academic Press*, San Diego, 1988.
- [23]. M. Okutan, E. Basaran, H. I. Bakan, F. Yakuphanoglu, AC conductivity and dielectric properties of Co-doped TiO<sub>2</sub>, *Physica B*, Vol. 364, 2005, pp. 300-305.
- [24]. A. Khelfa, N. Benramdane, J. P. Guesdon, C. Julien, AC conductivity of amorphous indium-selenium films, *Semicond. Sci. Technol.*, Vol. 9, 1994, pp.1-4.
- [25]. A. M. A. El-Barry, H. E. Atyia, Dielectric relaxation and AC conductivity of XS (X=Cd, Zn) compounds, *Physica B*, Vol. 368, 2005, pp. 1-7.
- [26]. A. Ghosh, Transport properties of vanadium germinate glassy semiconductors, *Phys. Rev. B*, Vol. 42, 1990, pp. 5665-5676.
- [27]. M. Pollak, T. H. Geballe, Low-Frequency conductivity due to hopping processes in silicon, *Phys. Rev.*, Vol. 122, 1961, pp. 1742 - 1753.
- [28]. N. F. Mott, E. A. Davis, Electronic Processes in non Crystalline Materials, *Clarendon press, Oxford*, 1979.
- [29]. J. C. Peuzin, D. Gignoux, Physique des diélectriques avec problèmes et exercices corrigés, *EDP Sciences*, 2009.
- [30]. B. Hilczer, Elektrety i piezopolimery, *PWN*, Warszawa, 1992.
- [31]. A. Von Hippel, Dielectrics and waves, *Artech House, Boston London*, 1995.
- [32]. J. C. Mage, Origine des pertes dans les matériaux, *RGE*, Issue 7, 1991, p. 24.

2014 Copyright ©, International Frequency Sensor Association (IFSA) Publishing, S. L. All rights reserved. (<http://www.sensorsportal.com>)



**FOR CUSTOM APPLICATIONS YOU NEED A FLEXIBLE PARTNER.**

**SENSOR SOLUTIONS FROM E+E ELEKTRONIK.**

**E+E ELEKTRONIK®**  
YOUR PARTNER IN SENSOR TECHNOLOGY

**SENSORS AND TRANSMITTERS FOR HUMIDITY, CO<sub>2</sub>, FLOW AND AIR VELOCITY**

E+E Elektronik's sensor solutions are as individual as your applications. We develop and produce all of our sensors and transmitters for relative humidity, CO<sub>2</sub>, air velocity and flow. We can therefore be extremely flexible in our approach to customers' specific requirements. This is one of our strengths. Another is outstanding measurement accuracy, excellent long term stability and high manufacturing quality of our products. See for yourself. [www.epluse.com](http://www.epluse.com)